Artificial Intelligence Framework for Skin Cancer Detector

A. Silpa[1], Palapati Venkata Nithish[2], Perugu Sasank[2], Nellore Syam[2],
Manikela Pawan Sai Kumar[2]

[1]Assistant Professor, Dept. of ECE, Geethanjali Institute of Science and Technology, Nellore, Andhra Pradesh.

[2]UG Student, Dept. of ECE, Geethanjali Institute of Science and Technology, Nellore, Andhra Pradesh.

Abstract

The skin cancer disease detection and analysis are constrained by human's visual potential as it entirely depends on microscopic behaviour. The computer-based image reorganization schemes are implemented in accurate classification and identification of skin cancer diseases. Disease Detection operation is performed by k-mean clustering operation on captured real time skin lesion image. Once the detection has been done its features are extracted by Gray Level Co-occurrence Matrix (GLCM) based Texture features; discrete wavelet Transform (DWT) based low level features and Statistical Color features respectively. Generally, classification is done by SVM based approaches, but it is having the low accuracy towards texture features. To implement features based matching operation, an advanced artificial intelligence based Probabilistic Neural Networks (PNN) approach is adopted for classification. The proposed approach is implemented in MATLAB environment, and the accuracy of this methodology is much better that conventional approaches.

Keywords: Dermoscopy, Skin cancer detection, Discrete wavelet Transform, Gray Level Co-occurrence Matrix, Probabilistic Neural Networks

1. Introduction

For much of the twentieth century, human cancer was a complicated illness, primarily caused by the accumulation of various molecular alternations and genetic instability, which were accumulating over time [1]. Insufficient data exists to develop a kind of prediction approach to effective therapy based on present prognostic classifications and diagnostic methods, which do not accurately reflect cancer [2]. A large proportion of the anti-cancer [3] medicines now in use do not make a significant distinction between normal and malignant cells [4]. Additionally, cancer is often treated and detected too late, with particular attention being paid to the point at which cancer cells have already [5] metastasized and invaded other areas of the body, as in this case [6]. Skin malignancies are one of the most prevalent types of cancer in humans, and they are among the many different types of cancer [7]. Skin cancer is classified into two types: non-melanoma and melanoma [8], with the former being the more common (Merkel cell carcinomas, squamous cell, basal cell and so on). A melanoma is one of the deadliest types of skin cancer that, if left untreated, may be lethal [9]. If melanoma is detected in its early stages, it has a good chance of being cured; nonetheless, advancing melanoma is fatal [10]. You can see the numerous forms of skin cancer lesions, including nerves, dermatofibroma, melanoma, vascular lesions, pigmented browns, pigmented benign keratoses, and basal carcinoma, to name a few examples.

2. Literature Survey

Utami, Ema, et al. (2022) [11] optimized the Random Forest classification in predicting LSD with Genetic Algorithm (GA) as a hyperparameter tuning and using SMOTE as a resampling technique for unbalanced datasets. Hurtado, Jairo, et al. (2021) [12] proposed a novel skin cancer classification system that works on images taken from a standard camera and studies the impact on the results of the

smoothed bootstrapping, which was used to augment the original dataset. Eight classifiers with different topologies (KNN, ANN and SVM) were compared, with and without data augmentation, showing that the classifier with the highest performance as well as the must balance one was the ANN with data augmentation, achieving an AUC of 87.1%, which saw an improvement from an AUC of 84.3% of the ANN trained with the original dataset. Jain, S., Singhania, et al. (2021) [13] performed a comparative analysis of six different transfer learning nets for multiclass skin cancer classification by taking the HAM10000 dataset. We used replication of images of classes with low frequencies to counter the imbalance in the dataset. The transfer learning nets that were used in the analysis were VGG19, InceptionV3, InceptionResNetV2, ResNet50, Xception, and MobileNet. Goceri, Evgin., et al. (2021) [14] aimed to present an analysis of recent applications proposed for automated detection of skin cancer and future potentials to assist the investigators in developing efficient methods to achieve accurate, objective, and early detection of the disease. Banasode, Praveen, et al. (2021) [15] proposed an easy way to detect the disease and help us to know before something turns out to be serious. The aim of this work is to detect skin cancer. People can get to know what skin disease they are having and what all precaution and measures to be taken at an early stage and it will help in treating the disease successfully. The major causes of skin cancer are air pollution, UV radiation, unhealthy lifestyle etc. The concept of machine learning will be used to determine the disease and help us to detect the result. The most used classification algorithms are supporting vector machine (SVM).

Rashid, Javed, et al, (2022) [16] proposed a novel deep transfer learning model for melanoma classification using MobileNetV2. The MobileNetV2 is a deep convolutional neural network that classifies the sample skin lesions as malignant or benign. The performance of the proposed deep learning model is evaluated using the ISIC 2020 dataset. The dataset contains less than 2% malignant samples, raising the class imbalance. Various data augmentation techniques were applied to tackle the class imbalance issue and add diversity to the dataset. Shah, Mitt. et al. (2021) [17] proposed to train the neural networks on low-resolution images. We then propose a fast, scalable, and efficient Deep Convolutional Neural Network, LRNet for skin cancer classification on low-resolution images. LRNet is trained on 10015 pigmented lesion images belonging to the HAM10000 dataset. The proposed model is also deployed to a publicly available web application. Bechelli, Solene, et al. (2022) [18] proposed to further assess the performance of DL models, we test them on a larger and more imbalanced dataset. Metrics, such as the F-score and accuracy, indicate that, after fine-tuning, pre-trained models perform extremely well for skin tumor classification. Abdar, M., et al. (2021) [19] proposed dynamic model enables us to use different UQ methods and different deep neural networks in distinct classification phases. So, the elements of each phase can be adjusted according to the dataset under consideration. In this study, two best UQ methods (i.e., DE and EMC) are applied in two classification phases (the first and second phases) to analyze two well-known skin cancer datasets, preventing one from making overconfident decisions when it comes to diagnosing the disease. Cheong, Kang Hao, et al. (2021) [20] proposed ASMD was employed to examine 600 benign and 600 DD malignant images from benchmark databases. Our classification performance assessment indicates that the combination of Support Vector Machine (SVM) and Radial Basis Function (RBF) offers a classification accuracy of greater than 97.50%. Motivated by these classification results, we also formulated a clinically relevant MI using the dominant entropy features. Our proposed index can assist dermatologists to track multiple information-bearing features, thereby increasing the confidence with which a diagnosis is given.

Rest of the paper is organized as follows: Section 2 details about literature survey, section 3 details about the proposed methodology, section 4 details about the results with discussion, and section 5 concludes article with references.

3. Proposed Methodology

The basic operational detail of the skin cancer disease detection and classification is represented in figure 1. Disease Detection operation is performed by k-mean clustering operation on captured real time skin lesion image. Once the detection has been done its features are extracted by GLCM based Texture features; DWT based low level features and Statistical Color features respectively. To implement features based matching operation, an advanced artificial intelligence based PNN approach is adopted for classification.
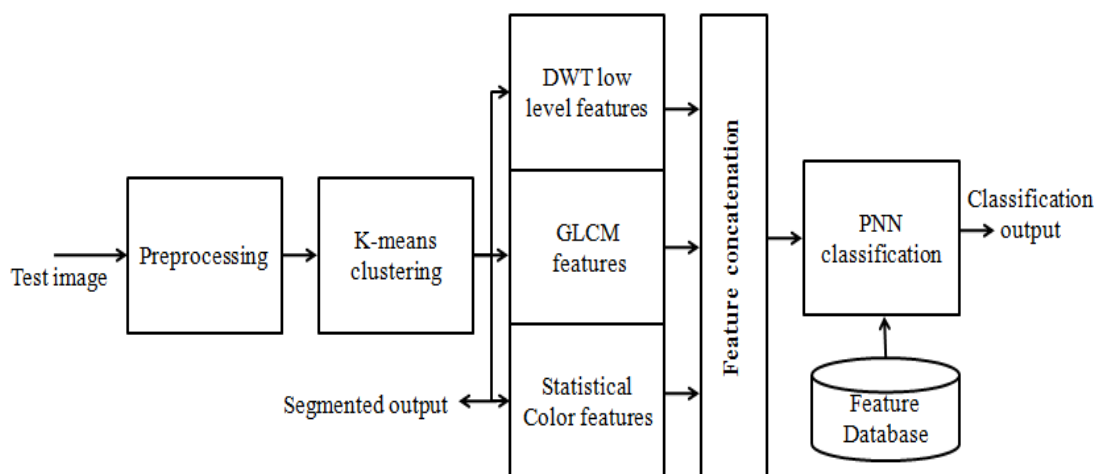
Figure 1. Architectural diagram of proposed system.

3.1 Preprocessing

Performing this step enhances the quality of the collected photos before they can be subjected to additional examination. Noise is defined as any undesirable information that may readily contaminate photographs. Almost all images and videos have some level of noise that significantly lowers the overall quality of the picture. Difficulty producing different types of noise may be caused by a variety of common causes, including specks of dust on or within the camera's lens, malfunctioning CCD parts in digital cameras, and other factors. It may also arise because of noisy sensors or transmission channel faults. A picture that has been damaged by various types of noise is an issue that occurs regularly in the capture and transmission of images. The noise arises from either the noisy sensors or from transmission faults caused by the channel. Listed below are the many sorts of noise that might be encountered. In addition to impulse noise (also known as salt and pepper noise), there is also gaudiasism (also known as white noise), speckle or multiplication, and periodic noise.

Impulse Noise

The impulse noise is also called as salt and pepper noise. It is caused by sharp, sudden disturbances in the image signal. Its appearance is randomly scattered white or black (or both) pixels over the image. For an 8-bit image, the typical value for pepper noise is 0 and for salt noise 255. In image and video processing, images are often corrupted by impulse noise. In this thesis, most popular methods are used to remove impulse noise such as median filter, mean filter, and wiener filter. Performances of the

median filter, mean filter and wiener filter are evaluated using the peak signal-to-noise ratio (PSNR), which is defined as

$$PSNR = 10\log_{10} \frac{255^2}{MSE}$$

(1)

Where MSE is the mean squared error (MSE)and defined as

$$MSE = \frac{1}{RC} \sum_{r=1}^{R} \sum_{c=1}^{C} (s[r,c] - y[r,c])^2$$

(2)

Here, s[r,c] and y[r,c] represent the original and the restored versions of a corrupted test image, respectively.

3.2 Image Segmentation

The image obtained by wireless IP camera is a RGB color components and it is a device-dependent color space. To find the defects of the images, they had to be transferred to the device-independent color space. In the device-dependent color space, the resultant color depends on the equipment employed to produce it, whereas in a device-independent color space, the coordinates specify the color and produce the same color regardless of the device used to draw it. Therefore, L*a*b* was developed as the device-independent color space transformation. The k-means clustering algorithm includes the following steps. The acquired skin cancer image is stored in RGB color space. It is a device dependent color space; the resultant color depends on the equipment employed to produce it. The L*a*b* is a device independent color space, in which the coordinates specify the color and produce the same color regardless of the device used to draw it and it is derived from human perception. In order to transform RGB color space into L*a*b* color space, first we extracted R, G, B component separately. After that RGB color space is transformed into CIEXYZ color space using the following formula

$$X = 0.4124 * R + 0.3576 * G + 0.1805 * B$$

$$Y = 0.2126 * R + 0.7152 * G + 0.722 * B$$

$$Z = 0.0193 * R + 0.1192 * G + 0.9505 * B$$

(3)

In L*a*b* colour space L* indicates the brightness factor, a* indicates the red or green content and b* denotes the yellow or blue content. Conversion RGB colour space into L*a*b* colour space using the following formula,

$$L* = 0.2126 * R + 0.7152 * B + 0.0722 * B$$

(4)

$$a* = 1.4749 *(0.2213 * R - 0.3390 * G + 0.1177 * B) + 128$$

$$b* = 0.6245*(0.1949 * R + 0.6057 * G - 0.8006 * B) + 128 \qquad (5)$$

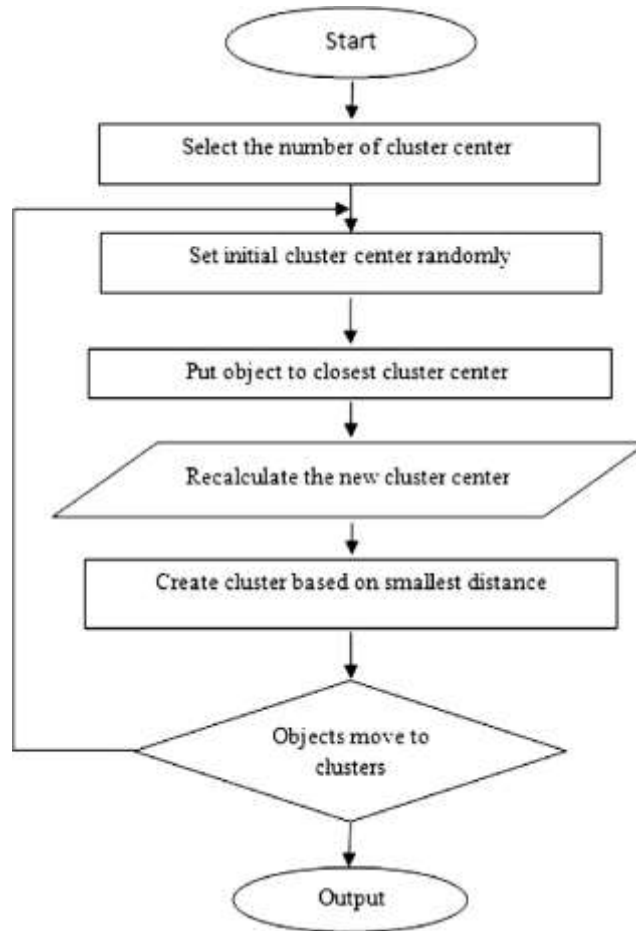In this method RGB colour space can be transformed into L*a*b* colour space

Figure 2. K-means Clustering

Image segmentation is the process of dividing the image into multiple clusters based on the region of interest presented to detect skin cancer. Regions of interest are a portion of skin images, which are used by radiologists to detect abnormalities like micro classifications (benign and malignant).

K means clustering is used in the proposed procedure for segmentation to a certain extent than Active counter clustering approach because of its speed of operation with maintaining the highest accuracy. K means clustering procedure combines the properties of jointly possibility and K means clustering approaches as shown in figure 2. Here the membership functions are generated in a probability-based manner to gets better detection. Among those detected tumors, the highest accurate cancer regions were considered as ROI.   The automatic extraction of ROI is difficult. So, ROIs are obtained through possibility cropping, which are based on location of abnormality of original test images. Here the membership functions are generated in a probability-based manner to gets better detection. Among those detected Cancer regions, the highest accurate Cancer region is considered as ROI.

3.3. Feature Extraction

At this stage of the work, we calculate the GLCM of an image to extract the set of features required for further calculations. In an arithmetical and statistical texture approach, texture consistency features are calculated based on the statistical geometric allocation for intensity of pixel at a known location comparative to another pixel in the image matrix. Based on the number of dots or pixels in each arrangement, it comprises of multi-order statistic features such as primary-order statistic features, subsequent-order statistic features and superior-order statistic features. Spatial dependence-based Texture and statistic Feature extraction using GLCM is the subsequent -order information, it will be utilized to analysis the picture as texture entity. GLCM is a group of spatial frequency entities or how repeatedly a grouping of image brightens contrast standards in pixel occurrences. Altering the contribution information into the group of spatial and texture statistic features is described as feature *extraction*.

GLCM features used are

$$\text{Contrast} = \sum_{a,b=0}^{N-1} S_{a,b} (a-b)^2 \tag{6}$$

$$\text{Homogeneity} = \sum_{a,b=0}^{N-1} \frac{S_{a,b}}{1+(a-b)^2} \tag{7}$$

$$\text{Correlation} = \sum_{a,b=0}^{N-1} S_{a,b} \left[\frac{(a-\mu_a)(b-\mu_b)}{\sqrt{(\sigma_a^2)(\sigma_b^2)}} \right] \tag{8}$$

$$\text{Angular Second Moment (ASM)} = \sum_{a,b=0}^{N-1} s_{a,b}^2 \quad \text{and Energy} = \sqrt{ASM} \tag{9}$$

Then, 2 level DWT is also used to extract the low-level features. Initially on the on the on the on the on the on the segmented output DWT is applied, it will results the output as the LL1, LH1, HL1 and HH1 bands respectively. Then entropy, energy and correlation features are calculated on the LL band. Then, on the LL output band again DWT is applied, and results the output as LL2, LH2, HL2 and HH2 respectively. Again entropy, energy and correlation features are calculated on the LL2 band respectively as shown in figure 4.
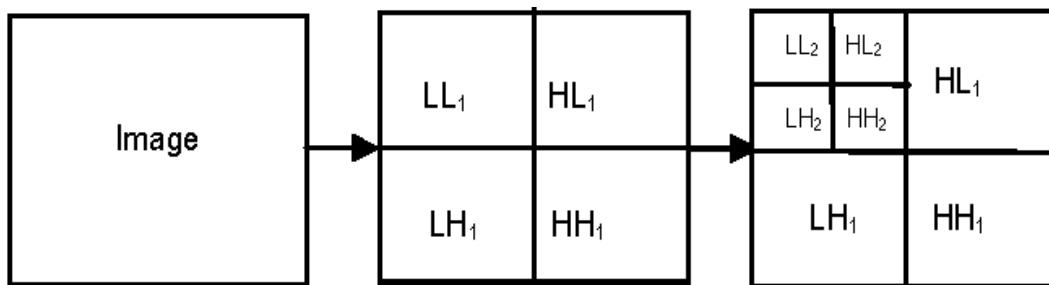

Figure 3. level DWT coefficients

And finally, Mean, and standard deviation based Statistical Color features are extracted from the segmented image. They are

$$\text{Mean } (\mu) = \frac{1}{N^2} \sum_{i,j=1}^{N} I(i,j) \tag{10}$$

$$\text{Standard Deviation } (\sigma) = \sqrt{\frac{\sum_{i,j=1}^{N} [I(i,j)-\mu]^2}{N^2}} \tag{11}$$

Then all these features are combined using array concatenation and results the output as hybrid feature matrix.

3.4. Classification using PNN

Figure 2 represents the detailed architecture of Training and Testing process using PNN. In the training process, on the skin cancer image dataset consisting of more than 1000 images are performed. In this training process, initially pre-processing operation will perform for noise removal then enhancements, segmentation operation to detect the location of disease using k means clustering then detected location features are extracted using GLCM filter.
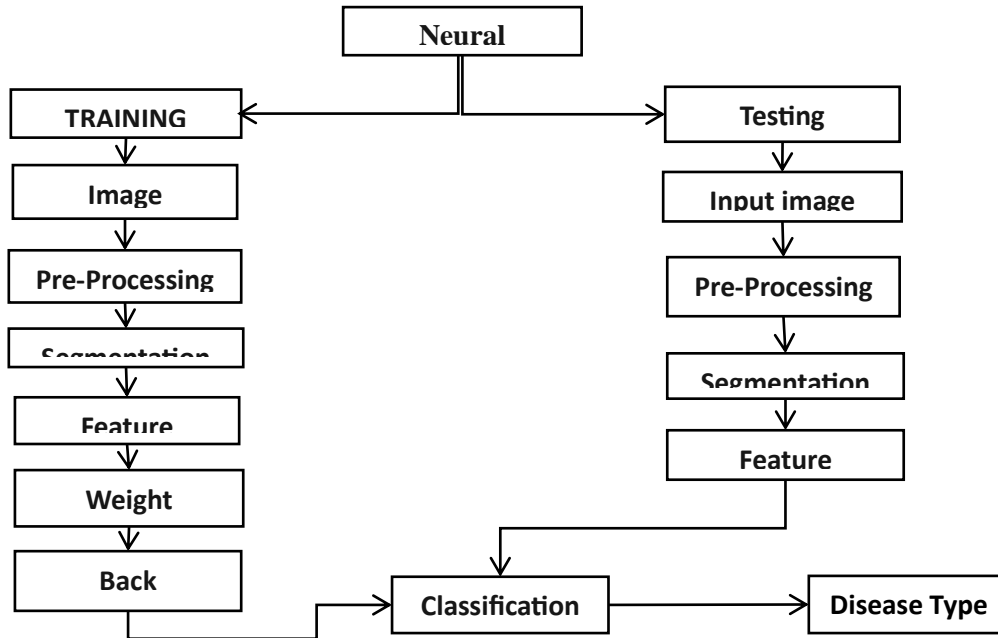

Figure 4. Proposed skin cancer skin lesion detection and classification system

Now the detected features are applied to weight adjustment process to create a sigmoid based model function for PNN back propagation model. The weights are altered based on the chronological relationship base on the multiple skin cancer diseases. Then using these weights an artificial intelligence based back propagation model will be formed. Whenever test image applied, its GLCM features are compared with the back-propagation model and classification operation will be formed. And classification results generate the type of disease with high accuracy. The major building block of Figure 5 is the PNN, which is used for classification purpose. It is an artificial intelligence-based approach consisting of neurones as its processing elements. These neurones hold the weight maps to solve the critical issues and classify the diseases. To implement this weight distributions, it is majorly depending on training operation on bulk amount of dataset. Thus, using this trained information, a random test objects either image or data will be applied on it. This operation is described as data classification or pattern identification. Training and Testing in image processing based digital environments; it requires the weight adjustments and its synaptic interconnections. The different combinations of weights will create the layer-based architecture as shown in Fig 3. The three major layers are Input, Hidden and Output layer.
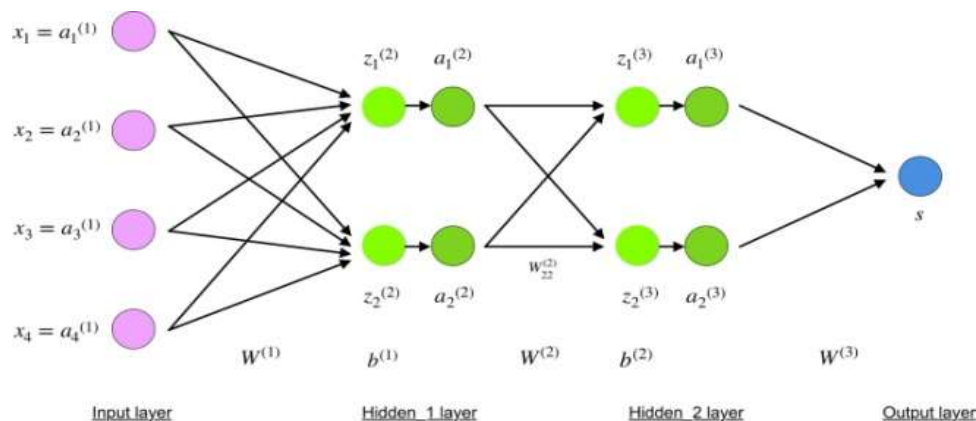
Figure 5. Back propagation model of PNN

Input layer: Every Weight map in the layer consists of predicted value. The input texture features are organized as a weight matrix here. As different types of texture features for different diseases are organized to create the weight model. Here x1, x2, x3, x4 can be treated as the different GLCM features, similar features from different diseases are grouped and fed to hidden layer.

Hidden layer: it is multi-layer architecture, here back propagation-based RBF kernel matrix will be created to classify the input layer information. Here a sigmoid control model will used to generate the weight matrix elements and its interconnections. Now, this weight matrix was created based on the similarity between the same categories of disease dataset of GLCM features, the similarity will be calculated by Euclidean distance criteria. Also, for different datasets of diseases relationship also identified here, to examine the test image features very precisely. If the test image features are matched with the more than one classification, then sigmoid control based back propagation model gives the accurate outcomes.

Output layer: the output layer holds the classification outcome pattern; thus, it compares the hidden layer output pattern with the original training data set pattern, so it will identify its accuracy, sensitivity and specificity. By the parallel procedure of all layers will generate the effectual categorization outcome.

4. Results and Discussions

For simulation purpose four different categories of skin cancer skin lesion are considered and trained using PNN through MATLAB R2018a simulation environment.

4.1 dataset

The experiments are done using the Matlab Programming language, and classification is done using the Matlab R2018a tool. ISIC is one of the biggest available collections of quality controlled dermoscopic images. For the implementation of the proposed method, spatial domain, and frequency domain of 30 dermoscopic skin lesion images (15-benign and 15-Malignant) have been obtained respectively by applying rotations at different angles. Train images of each label have been used to train the PNN architecture with fifty Epochs, whereas the remaining twenty percent is used for testing. The features extracted by GLCM; DWT future network are used to train PNN classifier to classify the images into its respective classes. The efficiency of the model can be computed using various performance metrics.

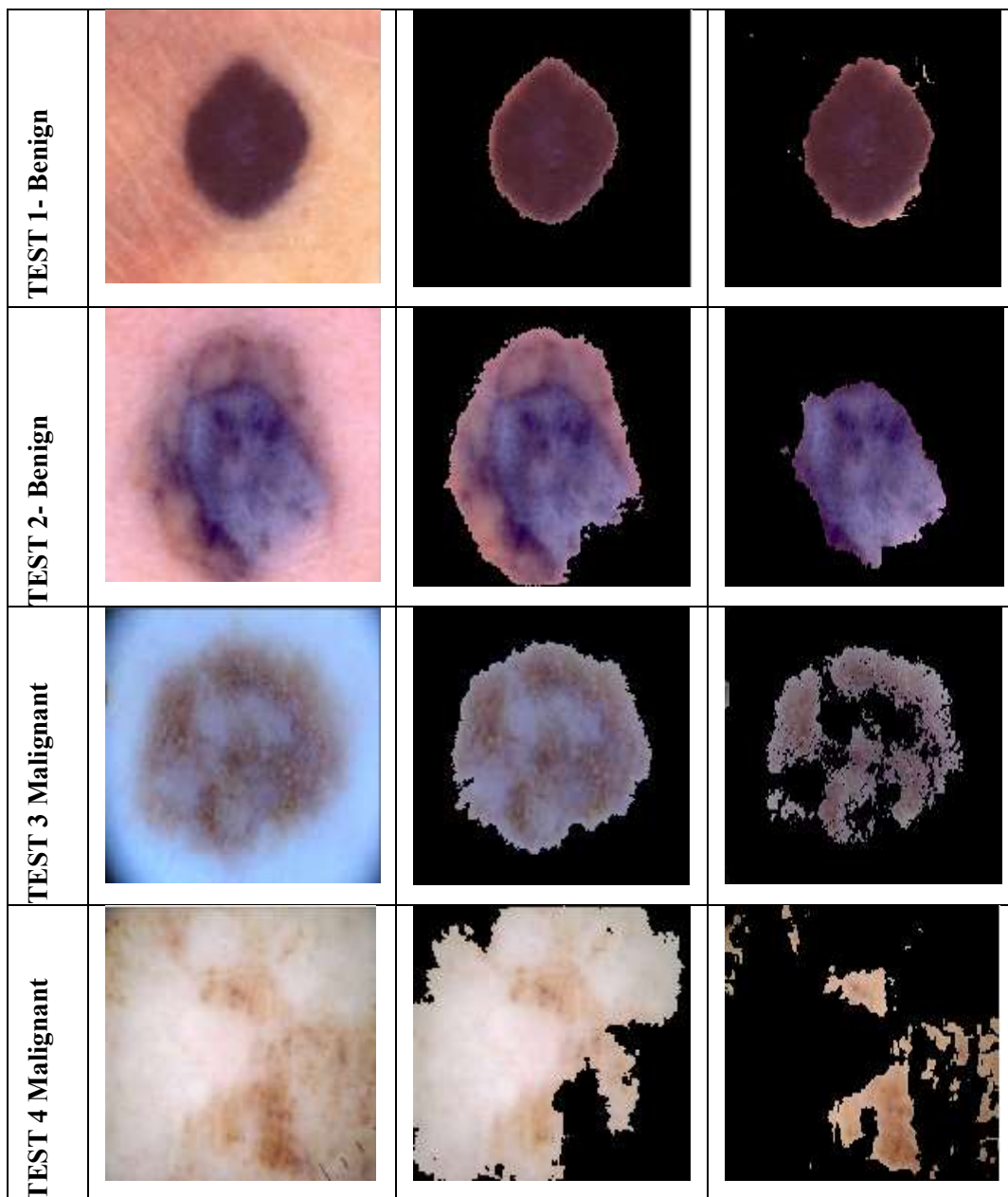|	Input image	Active contour segmented output	K-means segmented output

Figure 6: segmented output images of various methods

From figure 6, it is observed that the proposed method can be effectively detecting the regions of skin cancers, it indicates the segmentation done very effectively compared to the Active contour approach. Here, TEST-1 and TEST 2 images are considered benign, and TEST-3 and TEST-4 images are considered malignant type images respectively. For the malignant images, the segmentation accuracy is more.

4.2 Performance metrics

For evaluating the performance measure the proposed method is implemented with the two types of segmentation methods, they are Active contour (AC) and k-means clustering respectively. For performing this comparisons Accuracy, Sensitivity, F measure, Precision, MCC, Dice, Jaccard and Specificity parameters are calculated respectively.

Table 1. performance comparison

Metric	method	Test 1	Test 2	Test 3	Test 4
Accuracy	PNN-AC	0.9157	0.78099	0.85796	0.47765
	PNN-kmeans	0.99985	0.99715	0.99999	0.99999
Sensitivity	PNN-AC	0.70588	0.90024	0.9166	0.83857
	PNN-kmeans	0.99931	0.99198	1	1
F measure	PNN-AC	0.82207	0.68494	0.79395	0.44602
	PNN-kmeans	0.99965	0.99381	0.99998	0.99998
Precision	PNN-AC	0.98404	0.55275	0.70023	0.30381
	PNN-kmeans	1	0.99852	0.99997	0.99997
MCC	PNN-AC	0.7869	0.56857	0.70305	0.1835
	PNN-kmeans	0.99956	0.99198	0.99998	0.99998
Dice	PNN-AC	0.82207	0.68494	0.79395	0.44602
	PNN-kmeans	0.99965	0.99381	0.99998	0.99998
Jaccard	PNN-AC	0.69789	0.52085	0.65831	0.28702
	PNN-kmeans	0.99931	0.9877	0.99997	0.99977
Specificity	PNN-AC	0.99564	0.73812	0.83298	0.35685
	PNN-kmeans	1	0.99956	0.99999	0.99998

From Table 1 and Figure 6, it is observed that the proposed K-means clustering method along with PNN gives the highest performance for all metrics compared to the Active counter method.

Table 2. Accuracy comparison

Method	Test 1	Test 2	Test 3	Test 4
SVM-Linear kernel [14]	0.4	0.40	0.7	0.7
SVM-RBF kernel [14]	0.4	0.45	0.55	0.6
SVM-Polynomial kernel [14]	0.4	0.3667	0.50	0.5667
SVM-5 fold cross validation [14]	0.6	0.55	0.60	0.45
Proposed PNN-AC	0.9157	0.78099	0.85796	0.47765
Proposed PNN-K-means	0.99985	0.99715	0.99999	0.99999

From the Table 2, it is observed that the proposed method gives the highest accuracy for both Benign and malignant diseases compared to the various kernels of SVM [14] such as SVM-Linear kernel, RBF kernel; Polynomial kernel and 5-fold cross validation respectively.

5. Conclusion

This paper described a computational technique for the identification and classification of skin cancer using magnetic resonance imaging pictures, which was based on a PNN-based deep learning approach. In this case, Gaussian filters are used for preprocessing, which removes any undesirable noise components or artefacts that were introduced during the picture capture process. Then, for ROI extraction and cancer cell identification, K-means clustering segmentation is used in conjunction with segmentation. Then, for the extraction of statistical, color, and texture characteristics from segmented images, a GLCM and DWT based technique was devised, which was then tested. Finally, a trained network model was used to categories the kind of cancer, which might be either benign or malignant, using the PNN technique. As a result, after comparing PNN to other state-of-the-art methods, we determine that it is superior to the standard SVM approach. In the future, this study may be expanded by including a higher number of network layers into the PNN, and it may also be used to other types of malignancies, both benign and malignant, in the future.

References

[1] Tumpa, Priyanti Paul, and Md Ahasan Kabir. "An artificial neural network baseddetection and classification of melanoma skin cancer using hybrid texture features." Sensors International 2 (2021): 100128.

[2] Adegun, A., & Viriri, S. (2021). Deep learning techniques for skin lesion analysis and melanoma cancer detection: a survey of state-of-the-art. Artificial Intelligence Review, 54, 811841.

[3] Malo, D. C., Rahman, M. M., Mahbub, J., & Khan, M. M. (2022, January). Skin Cancer Detection using Convolutional Neural Network. In 2022 IEEE 12th Annual Computing and Communication Workshop and Conference (CCWC) (pp. 0169-0176). IEEE.

[4] Felmingham, Claire M., et al. "The importance of incorporating human factors in the design and implementation of artificial intelligence for skin cancer diagnosis in the real world." American Journal of Clinical Dermatology 22.2 (2021): 233-242.

[5] Malibari, Areej A., et al. "Optimal deep neural network-driven computer aided diagnosis model for skin cancer." Computers and Electrical Engineering 103 (2022): 108318.

[6] Agrahari, P., Agrawal, A., & Subhashini, N. (2022). Skin cancer detection using deep learning. In Futuristic Communication and Network Technologies: Select Proceedings of VICFCNT 2020 (pp. 179-190). Springer Singapore.

[7] Sannigrahi, Anindyadeep, et al. "Diagnosis of Skin Cancer Using Feature Engineering Techniques." 2021 3rd International Conference on Advances in Computing, Communication Control and Networking (ICAC3N). IEEE, 2021.

[8] Khamparia, Aditya, et al. "An internet of health things☐driven deep learning framework for detection and classification of skin cancer using transfer learning." Transactions on Emerging Telecommunications Technologies 32.7 (2021): e3963.

[9] Rajput, Gunjan, et al. "An accurate and noninvasive skin cancer screening based on imaging technique." International Journal of Imaging Systems and Technology 32.1 (2022): 354-368.

[10] Thurnhofer-Hemsi, Karl, and Enrique Domínguez. "A convolutional neural network framework for accurate skin cancer detection." Neural Processing Letters 53.5 (2021): 30733093.

[11] Utami, Ema, and Alva Hendi Muhammad. "Lumpy Skin Disease Prediction Based on Meteorological and Geospatial Features using Random Forest Algorithm with Hyperparameter Tuning." 2022 5th International Conference on Information and Communications Technology (ICOIACT). IEEE, 2022.

[12] Hurtado, Jairo, and Francisco Reales. "A machine learning approach for the recognition of melanoma skin cancer on macroscopic images." TELKOMNIKA (Telecommunication Computing Electronics and Control) 19.4 (2021): 1357-1368.

[13] Jain, S., Singhania, U., Tripathy, B., Nasr, E. A., Aboudaif, M. K., & Kamrani, A. K. (2021). Deep learning-based transfer learning for classification of skin cancer. Sensors, 21(23), 8142.

[14] Goceri, Evgin. "Automated skin cancer detection: where we are and the way to the future." 2021 44th International Conference on Telecommunications and Signal Processing (TSP). IEEE, 2021.

[15] Banasode, Praveen, Minal Patil, and Nikhil Ammanagi. "A melanoma skin cancer using machine learning technique: support vector machine." IOP Conference Series: Materials Science and Engineering. Vol. 1065. No. 1. IOP Publishing, 2021.

[16] Rashid, Javed, et al. "Skin cancer disease detection using transfer learning technique." Applied Sciences 12.11 (2022): 5714.

[17] Shah, Mitt. "LRNet: Skin Cancer Classification using Low-Resolution Images." 2021 International Conference on Communication information and Computing Technology (ICCICT). IEEE, 2021

[18] Bechelli, Solene, and Jerome Delhommelle. "Machine learning and deep learning algorithms for skin cancer classification from dermoscopic images." Bioengineering 9.3 (2022): 97.

[19] Abdar, M., Samami, M., Mahmoodabad, S. D., Doan, T., Mazoure, B., Hashemifesharaki, R., ... & Nahavandi, S. (2021). Uncertainty quantification in skin cancer classification using threeway decision-based Bayesian deep learning. Computers in biology and medicine, 135, 104418.

[20] Cheong, Kang Hao, Kenneth Jian Wei Tang, Xinxing Zhao, Joel En Wei Koh, Oliver Faust, Raj Gururajan, Edward J. Ciaccio, V. Rajinikanth, and U. Rajendra Acharya. "An automated skin melanoma detection system with melanoma-index based on entropy features." Biocybernetics and Biomedical Engineering 41, no. 3 (2021): 997-1012.